P15.336 PROGRESS IN MITIGATION OF WLAN INTERFERENCE AT WEATHER RADAR

Reino Keränen[1)], Laura Rojas[1,2)] and Petri Nyberg[1)]
[1)] Vaisala Oyj, [2)] University of Helsinki, Helsinki, Finland

1. INTRODUCTION

Artificial radio interference such as wireless/radio local area networks (WLAN/ RLAN) [IEEE802.11] have impacts on weather radar data quality. These networks are widely used, and they are often working in the same frequency bands as weather radars. Their emissions often contaminate the radar observations. Distinctly, the interference show up as persistent false echo taken as precipitation in fair weather. In addition, they may distort Doppler and dual-polarization measurements of the precipitation signal, and they may contribute to the ambient noise power which is a parameter in radar reflectivity calibration.

The management of WLAN/RLAN issues in weather radar is a diverse activity including the efforts to enforce general standards, such as dynamic frequency selection (DFS). Radar observations require continuous quality control for interference. Individual sources in daily operations can be localized for authorization processes. Eventually, means of mitigation have to be considered. Continuous, efficient monitoring and identification of the WLAN/RLAN interference in the radar data are key tools in all these activities.

WLAN/RLAN features have been investigated as signals injected to the radar receiver inputs, as well as single source emissions from the proximity of a radar site [Joe et al, 2005]. Aggregate effects of multiple WLAN/RLAN systems at further distances from the radar have been modeled [Tercero et al., 2011]. Temporal features of the WLAN/RLAN packet traffic have been considered in [Norváth and Varga, 2009] with proposals for improvements in the channel allocation policy of the WLAN/RLAN devices.

In weather radar, semi-static censoring maps are a generic tool of clutter mitigation – with the trade-off of observations lost in the areas covered by the interference. External observations such as satellite data can be applied as a mask, while their timely availability is a constraint. The thresholds on signal-to-noise ratios (SNR) can be increased to censor out weak interference, however, leading to systematic loss of the weak weather signal. The most harmful intense interference remain. Recently, a dual polarization fuzzy spectral filter was constructed to suppress the interference in radar data [Rojas et al, 2012]. The computationally demanding approach leads to a highly selective filter with a strong identification capability, while the variability of the dual-polarization signatures of WLAN/RLAN remains a challenge. Simple time domain filters [RVP900™] of the received voltages, originally constructed against pulsed signals from other radars, have been found to reduce the WLAN/RLAN interference in some cases.

In this study, we examined the features of WLAN/RLAN transmissions as seen by the weather radar, in order to understand further the existing methodologies and to improve the recognition of WLAN/RLAN interference. We reproduced the controlled 'in-lab' setup of WLAN/RLAN by [Joe et al., 2005] and extended the study of observed the 'bursts of power' and the spectra into the features of the received digitized complex voltages in time domain. We compared our findings with the standards [IEEE802.11] defining the communications. We recognized correspondences which are thus expected to be common to all the devices applying the particular protocol of communication. Such universality defines a robust basis for recognition of their presence in radar data, as automated approaches.

2. A SETUP FOR CONTROLLED WLAN/RLAN INPUT TO RADAR RECEIVER

The measurement set up consists of a network of two WLAN access point (AP) devices (D-Link DAP-2553) in the laboratory environment. The communications are configured to the bandwidth of 20 MHz at the channel 48 (5240 MHz). The transmissions are intercepted by a low gain monopole antenna. The antenna signals are converted to the pass band of the Vaisala weather radar receiver, centered to the AP channel 48, digitized and processed by the RVP900 Digital Receiver and Signal Processor [RVP900]. Agilent E4438C is used as a local oscillator. The streams of data transfer are generated between the Linux PCs by the *iperf* monitoring software. The block diagram of the setup is shown in Figure 1.

The AP devices are configured to transmission power +7dBm. The emissions from closer AP are observed by

[1] *Corresponding author address:* Reino Keränen, Vaisala Oyj, P.O.Box 26, FI-00421 Helsinki, FINLAND; emails: Reino.Keranen@vaisala.com, Laura.Rojas@vaisala.com, Petri.Nyberg@vaisala.com

the RVP900 at a typical signal-to-noise ratio (SNR) of 30 dB, while the transmissions from the second AP were observed at SNR of 10 dB. By accounting for the typical gains and losses, the setup roughly mimics an actual radar pointing steadily at WLAN/RLAN access points at short distances from hundreds meters to a few kilometers from the radar. The maximal throughput of the TCP data transfer was typically about 50 Mb/s, and UDP packets were communicated free of errors approximately at the same rate.

As expected, WLAN/RLAN transmissions generate bursts of variable power received at consecutive range times i.e. gate data sampled as rays of 80 pulses, shown in the range-time displays of power in Figure 2. At lower transmission rates, the bursts are distinct and have a minimal length of 20 μs. As soon as the WLAN/RLAN throughput is increased, the bursts turn semi-continuous. For transmissions at a fair fraction of the maximal capacity, the transmissions are observed at a continuous and relatively constant power, with some interruptions.

A study into the time series of received voltages in range and in pulse time reveals the intrinsic pattern of the WLAN/RLAN data frames. The apparent power that is summed from the ray pulses actually originates from individual or a fraction of pulses of remarkably large amplitudes, observed as spikes in the voltage time series in sample times, middle graphs in the screens in Figure 2. The typical individual pulse sequences in range time are consistent with the noise floor, interrupted by variable bursts of interference, as shown in the bottom of screens in Figure 2. These patterns persist as long as the throughput is well below the maximum capability. At the maximal throughput, the pattern is inverted i.e. the majority of pulses are 'WLAN/RLAN'-like, interrupted by the individual pulses of 'thermal noise'.

These features are, to a great extent, independent of the radar settings, such as the receiver band width matched to the pulse lengths typical in weather radar. The choice of pulse repetition frequency selects variable patterns in the WLAN/RLAN spike sequences in pulse-time. The patterns suggest that the spikes are not randomly distributed. However, the typical numbers of spikes sampled in ray are relatively stable and scale with the throughput. In rays computed from a large number of samples the probability is increased for occurrence of (a) spike(s), however the mean power remains reasonable. On the contrary, in ray data computed from few samples, the power bursts are stronger but less frequent. Towards higher throughputs transmissions the burst-like behavior of the mean power is sustained longer in rays of fewer samples than for higher number of samples.

3. BASICS OF WLAN/RLAN COMMUNICATIONS

The standards in the IEEE802.11 series [IEEE 802.11] govern the protocols used in WLAN/RLAN. Flat spectral characteristics follow from the concept of Orthogonal Frequency Division Multiplexing (OFDM) specified in versions of 802.11a, g and n [van Knee, 2007]. The OFDM uses thousands of parallel narrow band channels leading to relatively long symbol time of 4 μs, which defines the unit length of communication in time. The actual lower limit of data frame lengths result from the headers required for synchronization and for other management of transfers. In 802.11a/g, the headers are 20 μs in length, as shown in Figure 3a. 802.11n is compatible with them while extends them in Multiple Input Multiple Output (MIMO) approaches, as shown in Figure 3b. The communication includes periods of idle time due to the channel allocation checks, and/or due to Request-to-Send/Clear-to-Send cycles.

Practically, WLAN/RLAN devices that are compliant to the 802.11a,g,n standards i.e. share the common characteristics of "OFDM" lead to data communications in relatively long bursts starting from 20 μs upwards. The intrinsic overheads in the protocol prevent reaching the naïve maximum throughput. They impose interruptions, which show up as idle periods in the emissions. These standard properties largely explain the features observed in our controlled in-lab evaluations, which we may thus expect to be common to all "OFDM systems".

Certainly, conditions at actual radars may be complicated by the multiple sources, multipath features etc. However, the high directivity of radar antennas and the strong dependency of WLAN/RLAN signal strength as function of range tend to detect specific emissions. We note that the OFDM techniques are not limited to WLAN/RLAN applications, but they are in use or considered to be used in various wireless technologies, such as digital radio, TV and cellular networks. Furthermore, not all WLAN/RLAN apply OFDM. The acronym OFDM thus characterizes more accurately the category of interference considered in this study.

4. TREATEMENTS OF NON-RAYLEIGH COMPONENTS IN TIME SERIES OF THE RECEIVED WEATHER RADAR ECHO

Our first objective is to recognize OFDM emissions in the received voltages originating from weather echo, superimposed on the thermal noise floor. The statistical properties of precipitation echo and noise are universal. The received voltages are complex Gaussian, which implies that their squared amplitudes of voltages composed of precipitation echo and of thermal noise are Rayleigh distributed, at any SNR. Their distribution is parameterized by the expectation value of the received power. Precipitation echo are typically stationary within the rays.

In addition, the spectrum of the precipitation echo depends on the radial velocities of scatterers (Doppler radar), and the precipitation echoes are highly correlated in the orthogonal channels of dual-polarization radars,

while the spectrally flat thermal noise is uncorrelated between the channels. By conception, OFDM is spectrally flat while the correlations between dual-polarization channels remain unspecified by OFDM, i.e. may depend on contextual conditions. These general features are summarized in Table 1.

It is then evident that the OFDM emissions can be recognized in the radar data as deviations from the Rayleigh statistics. In its simplest form, pulse-to-pulse differences of the received amplitudes [RVP900™] have been considered with a criterion that they rarely exceed a level which corresponds to an acceptable rate of false recognitions (FAR) for Rayleigh signals. It is clear that this approach works as long as the OFDM spikes are separated from each other, which is the case when the communication throughput is well below its maximal capacity. The approach is very robust as it succeeds in non-stationary echoes. The method can be used as a filter in the limit of large spectral width, i.e. the pulses tagged as non-Rayleigh can be replaced by complex values consistent with Rayleigh while arbitrary in phase.

Given the increasing computing capacity, more rigorous tests of Rayleigh hypothesis can be conducted by considering larger sets of voltages that are piecewise stationary i.e. their power expectation value prescribes the distribution of their amplitudes. Standard statistical methods such as the χ^2 test can be applied to ray data gate-by-gate. The approach can be expected to recognize OFDM even if the spikes are frequent and clustered. It can be tested on cases of high WLAN/RLAN throughputs in which a large fraction of pulses in the sample are contaminated. A χ^2 test is simple enough for real-time uses. It has a small number of configurable parameters, which makes it well suited for validation and assessments of performance. The test can be carried out at any SNR and it can be repeated independently in the channels of dual-polarization.

Additionally, we are interested in filtering out the non-Rayleigh components by replacing the spiky entries with values that are consistent with the remaining part of the sample. This appears feasible by applying the models of 'noise' (i.e. flat spectrum) and of 'precipitation' (peaked spectrum) for estimating new amplitudes and phases for the entries to be replaced. The component of 'ground clutter' can be taken as a special narrow spectral width.

The quality can be managed consistently by reporting the presence of OFDM interference as gate specific flags, or cumulatively in ray summaries. For monitoring purposes, it is important to preserve the original state, for example as observations of uncorrected power. Figure 4 shows the block diagram of the process.

5. EVALUATIONS

We have implemented a prototype version of χ^2 test of the Rayleigh hypothesis in the RVP900™ signal processor [RVP900™], with subsequent filtering of non-Rayleigh components, as depicted in Figure 4. At each gate, the sample is declared tentatively non-Rayleigh if the χ^2 sum exceeds a threshold, which can be set to the 90% confidence level of the Rayleigh hypothesis, for example. For the suspicious gates, individual samples are flagged non-Rayleigh at the 95% confidence level, for example. If non-Rayleigh entries are found, the gate is confirmed non-Rayleigh, and the anomalous entries are replaced by estimates derived from the Gaussian model of noise and precipitation.

The performance of the method in mitigating OFDM transmissions in conditions of idle WLAN/RLAN and UDP data transfers at various rates are displayed in Figure 5. The background noise dominates in conditions of idle WLAN. The rare bursts of interference are fully removed in filtering. The interference occupy almost all the gate data as soon as UDP data are transferred at 1Mb/s. The underlying noise floor is fully recovered in this case as well as in the case of a high throughput of 30Mb/s. At the througput of 35 Mb/s, 98% of the gates are recognized as non-Rayleigh. The interference power is suppressed by 30 dB, restoring the original noise floors in majority of the gates. The last case corresponds to an aggressive case of OFDM interference in actual radar conditions.

We have evaluated the methodology on interference observed in time series recorded at operational radars, as displayed in Figure 6. In Belo Horizonte, Brazil, a persistent interference was observed in the vertical polarization channel of the WRM200 radar. It was later confirmed to originate from WLAN/RLAN. The Rayleigh test and filter suppresses the most intense parts of the interference. In New Delhi, India, several aggressive interference get suppressed in data acquired by the WRK200 radar. Similarly, persistent interference are significantly suppressed in the WRM200 radar located in Harku, Estonia.

6. CONCLUSIONS

Features in transmissions from WLAN/RLAN as intercepted by the weather radar may be associated with the specification standards of WLAN/RLAN, which makes them universal thus suggesting their automated recognition is feasible. In particular, the OFDM technique is widely used in 802.11a,g,n compliant WLAN/RLAN and in other wide band digital communications. Its signatures can be recognized as deviations from the Rayleigh statistics of the power of the received voltages.

At rates well below the maximum throughput, the OFDM transmissions show up as power spikes in pulse-time samples, which can be tagged by simple pulse-to-pulse considerations. Transmissions closer to the maximal throughput motivate more advanced tests of Rayleigh, which are simple enough for real-time implementation. Filtering can be applied through modeling the sampled

voltages as a combination of precipitation echo and thermal noise.

First evaluations of the prototyped real-time implementation in the RVP900™ signal processor indicate that OFDM interference can be recognized and even filtered in controlled conditions up to the transmission rates not far from the maximum throughput. In actual radar cases, sources of interference at variable strengths known to be WLAN/RLAN, or consistent with them, are significantly suppressed.

7. REFERENCES

IEEE 802.11™ Wireless Local Area Networks, the Working Group for WLAN Standards http://www.ieee802.org/11/#;

Paul Joe, John Scott, John Sydor, Andre Brandão and Abbas Yongacoglu. (2005): Radio Local Area Network (RLAN) and C-Band Weather Radar Interference Studies. *AMS, the 32nd Conference on Radar Meteorology,* Albuquerque, NM;

Miurel Tercero, Ki Won Sung and Jens Zander (2011): Impact of Aggregate Interference on Meteorological Radar from Secondary Users. *Proc. IEEE WCNC*, Cancun, Mexico, September 2011;

Zoltán Horváth and Dávid Varga. (2009): Elimination of RLAN interference on weather radars by channel allocation in 5 GHz band. *Proc. IEEE ICUMT International Conference on Ultra-Modern Telecommunications & Workshops*, St. Petersburg, Russia, October 2009;

Laura C..Rojas, Dmitri Moisseev, V. Chandrasekar, Jason Selzler, Reino Keränen. (2012). Dual-polarization spectral filtering for radio frequency interference suppression, *the 7th European Conference on Radar in Meteorology and Hydrology*, Toulouse, France, June 2012;

Richard van Nee, V.K. Jones, Geert Awater, Allert van Zelst, James Gardner and Greg Steele (2007): The 802.11n MIMO-OFDM Standard for Wireless LAN and Beyond. *Wireless Personal Communications* **37**, pp. 445–453;

RVP900™ Digital Receiver and Signal Processor, User's Manual ftp://ftp.sigmet.com/outgoing/manuals/

Property / Input	Power [SNR]	Pulse power statistics	Doppler spectrum	Co-polar correlation
WLAN/RLAN	Anything, varies rapidly, bursts	Irregular	Flat	Variable
Precipitation	Anything, varies slowly	Rayleigh	Variably peaked	High
Thermal noise	A small constant (+/- 2dB)	Rayleigh	Flat	Zero

Table 1. Features of the OFDM interference, precipitation and thermal noise.

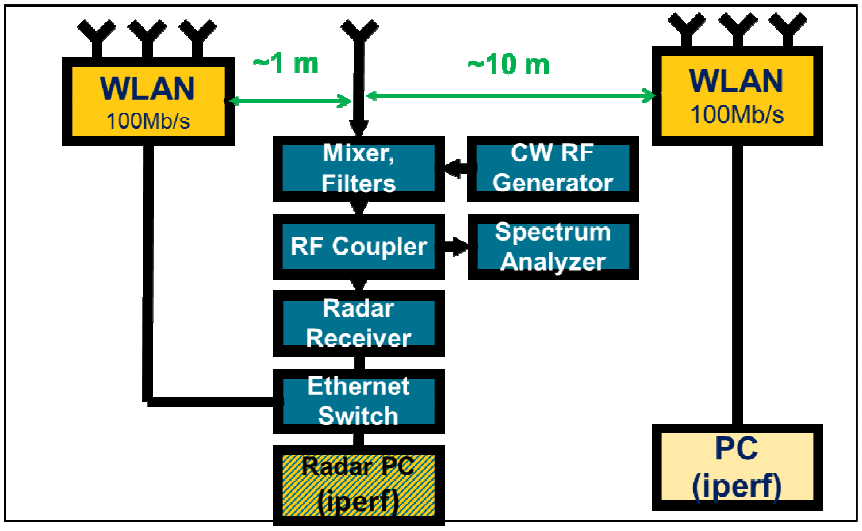

Figure 1. Block diagram of the set-up for the characterization of WLAN/RLAN interceptions.

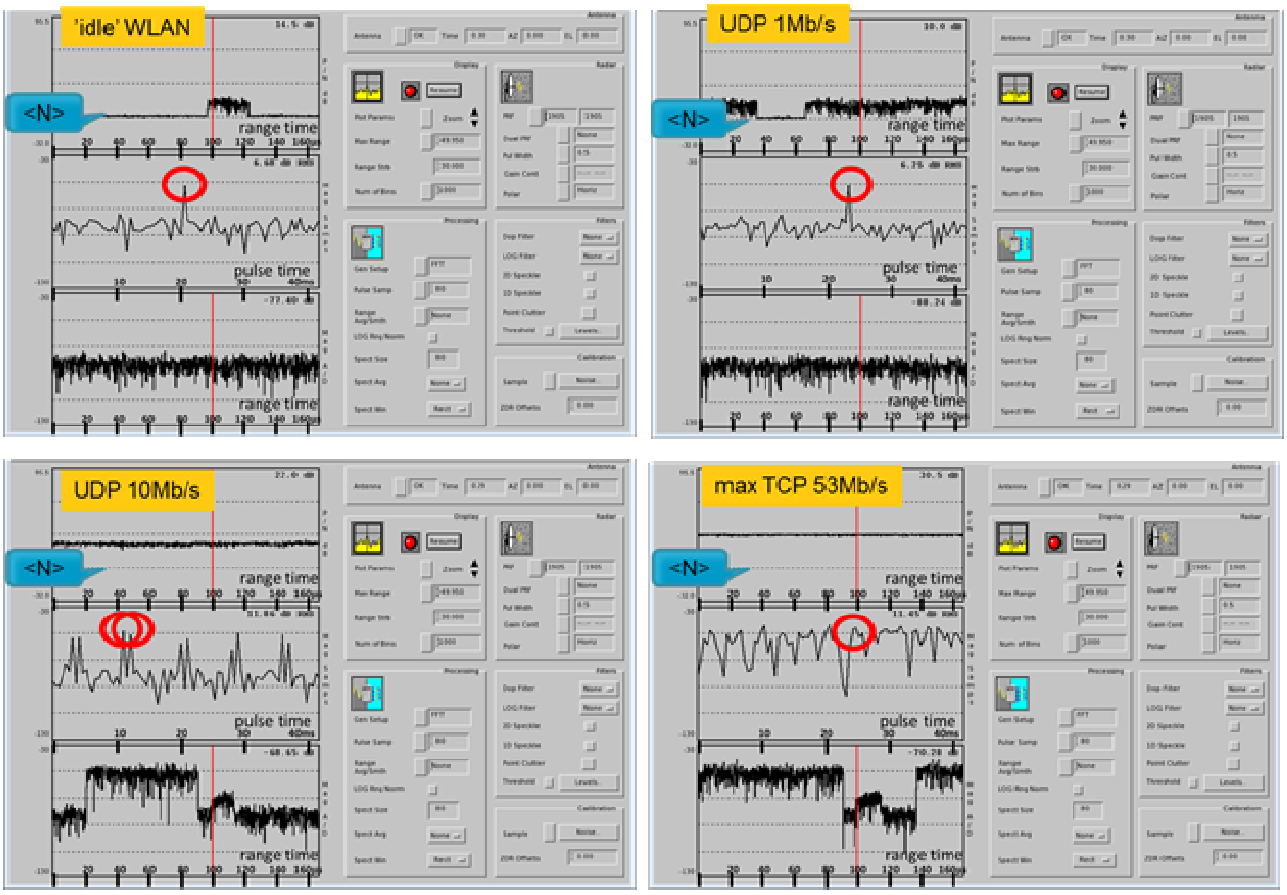

Figure 2. WLAN communications intercepted by the radar receiver. In each screen, the power estimates (P/N) from 80 samples are shown as function of the range-time (top), the amplitudes of the voltages in pulse-times at the gate marked with red (middle), and the amplitudes of the voltage time series in range-time (bottom). Upper left: idle WLAN, upper right: UDP at 1Mb/s, lower left: UDP at10Mb/s, lower right: max throughput of TCP/IP.

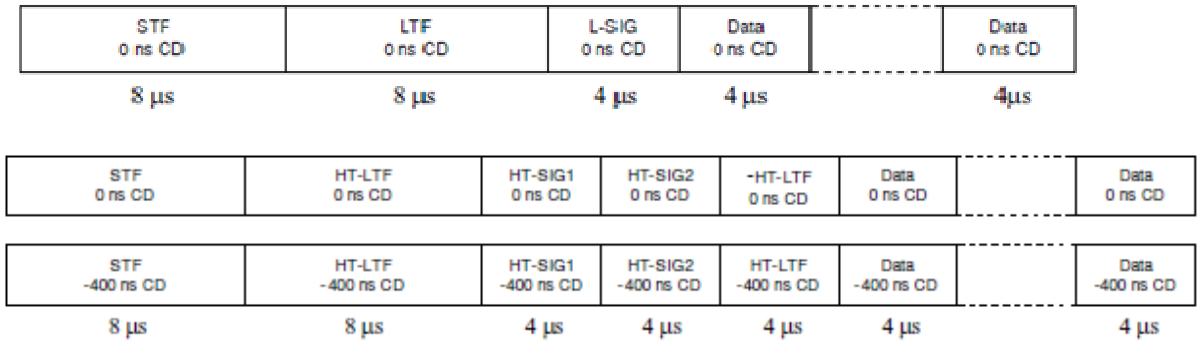

Figure 3. Top: the packet frame structure in the standards of IEEE802.11a,g. The first three frames are header frames of WLAN, followed by the data frames. All transfers are a multiple of symbol times of 4 µs with a minimum length of 20 µs. Bottom: the packet frame structure the standard of IEEE802.11n. Captured from [van Knee et al., 2007].

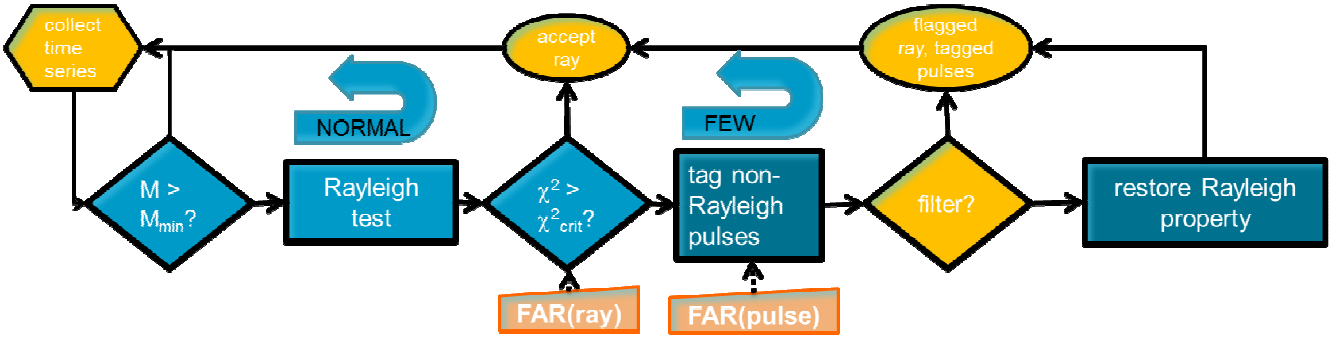

Figure 4. Block diagram for recognizing the presence of OFDM interference as a non-Rayleigh component in the received voltages squared. Subsequently, the anomalous pulses are tagged. Optionally, the non-Rayleigh component can be filtered out in time domain. The objects "FAR(ray)" and "FAR(pulse)" indicate the configurable parameters in the method. Computationally, the loop "NORMAL" dominates in absence of interference.

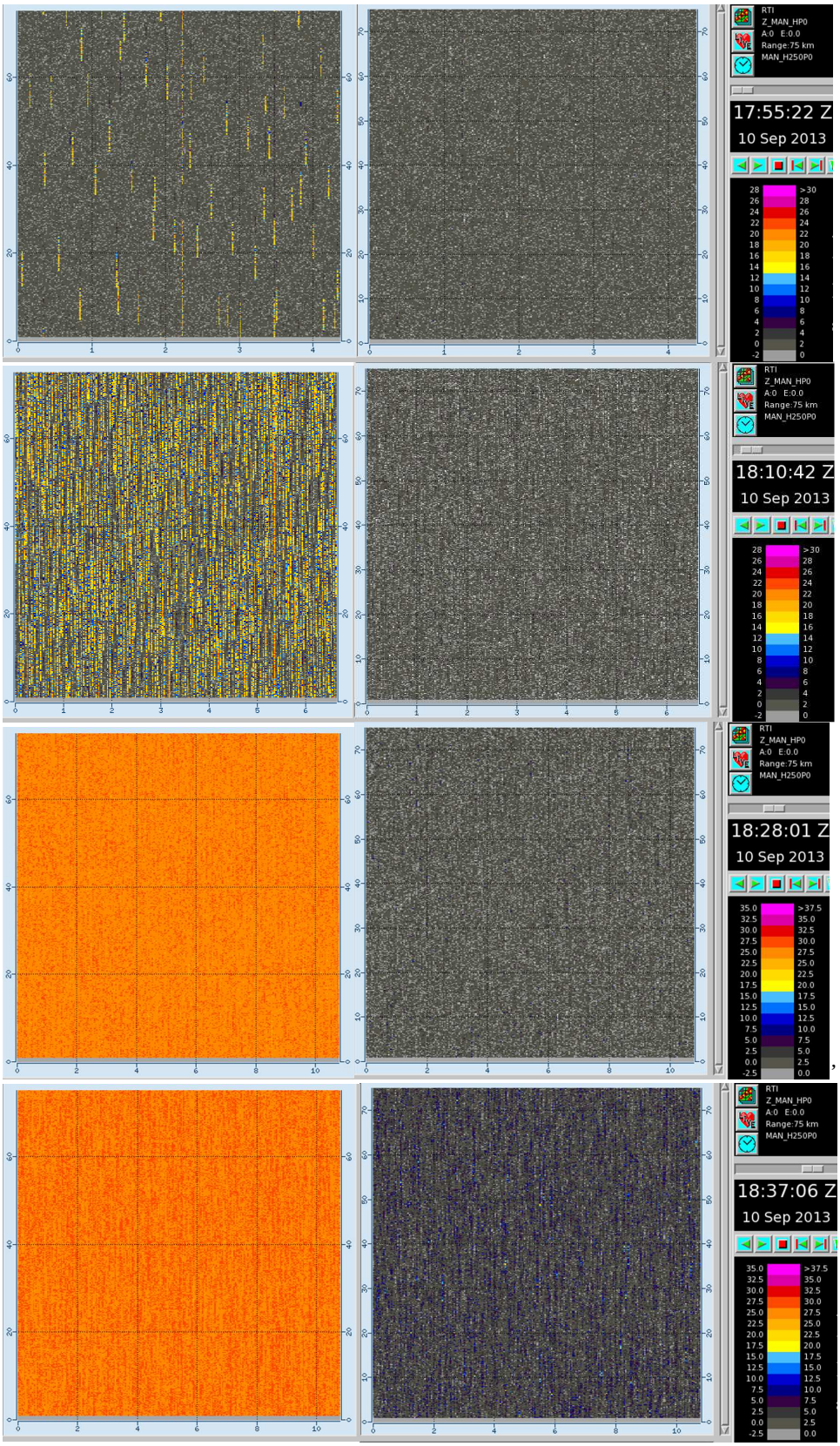

Figure 5. Range-time displays of the total sample powers (left) and sample powers, in which the non-Rayleigh components have been recognized and filtered out. Powers are expressed in units of P/N (dB). Top row: idle WLAN/RLAN network, 2nd row: UDP data transfer at 1 Mb/s, 3rd row: UDP data transfer at 30 Mb/s, bottom row: UDP data transfer at 35 Mb/s in the network capable to 50 Mb/s communications.

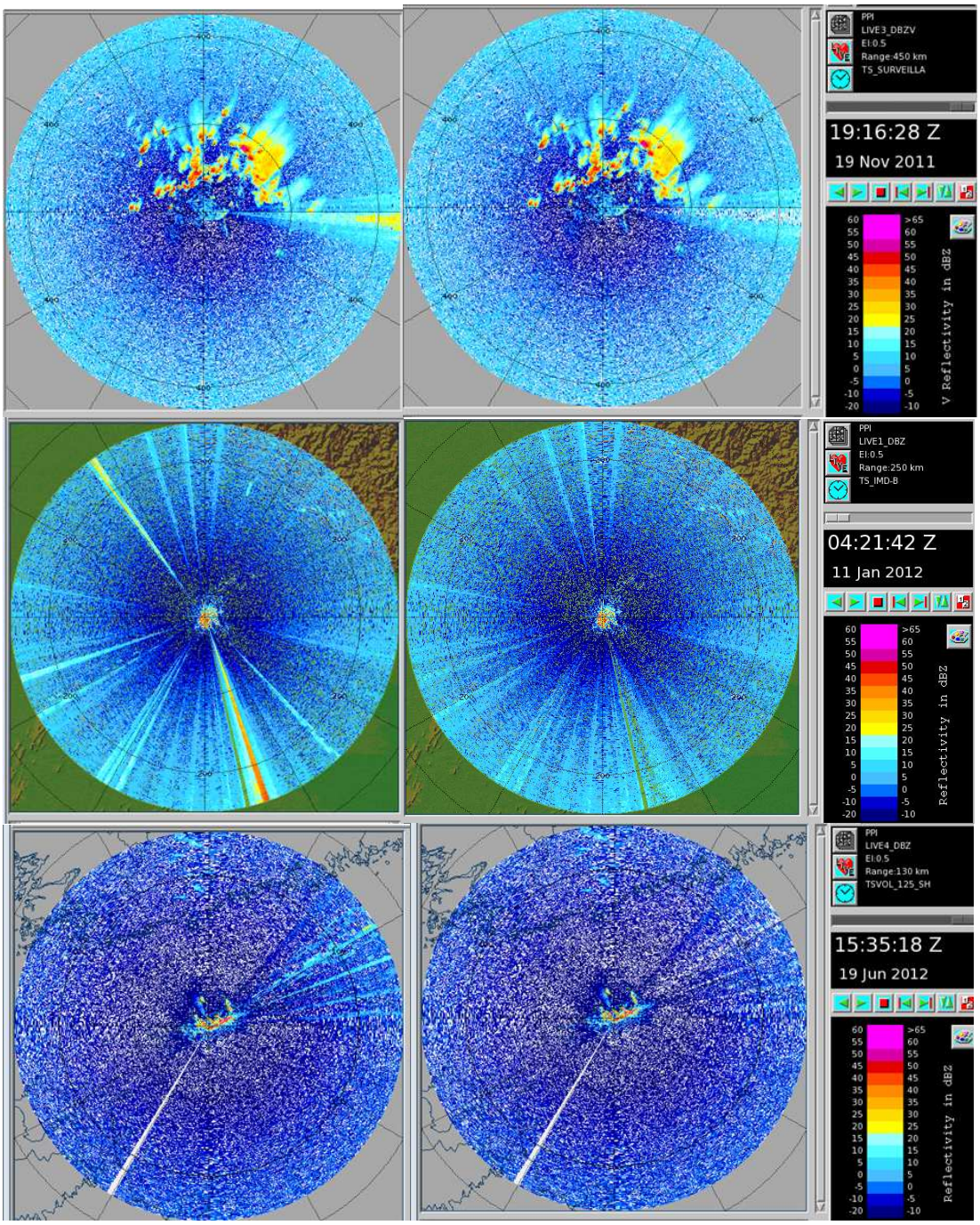

Figure 6. Field evaluations of the recognition and the filtering of radio interference based on Rayleigh testing. Left column: total power, right column: total power filtered for Rayleigh components, expressed in units of dBZ. Top row: a case of known WLAN/RLAN interference at the WRM200 radar in Belo Horizonte, Brazil. Middle row: a case of multiple aggressive radio interference at the WRK200 radar in New Delhi, India. Bottom row: a case of persistent radio interference at the WRM200 radar in Harku, Estonia. The white sector into South-West in the bottom row is a skipped ray.